Supplemental material to this article can be found at:
http://jpet.aspetjournals.org/content/suppl/2021/01/26/jpet.120.000229.DC1

1521-0103/377/1/1–10$35.00
THE JOURNAL OF PHARMACOLOGY AND EXPERIMENTAL THERAPEUTICS
Copyright © 2021 by The American Society for Pharmacology and Experimental Therapeutics
https://doi.org/10.1124/jpet.120.000229
J Pharmacol Exp Ther 377:1–10, April 2021

The Journal of PHARMACOLOGY And Experimental Therapeutics

Optimization of Lipophilic Metalloporphyrins Modifies Disease Outcomes in a Rat Model of Parkinsonism[S]

Li-Ping Liang, Ruth Fulton, Erica L. Bradshaw-Pierce,[1] Jennifer Pearson-Smith, Brian J. Day, and Manisha Patel

Department of Pharmaceutical Sciences, University of Colorado, Anschutz Medical Campus, Aurora, Colorado (L.-P.L., R.F., E.-L.B.-P., J.P.-S., B.J.D., M.P.) and Department of Medicine, National Jewish Health, Denver, Colorado (B.J.D.)

Received July 17, 2020; accepted January 19, 2021

ABSTRACT

Oxidative stress plays a crucial role in the pathogenesis of Parkinson disease (PD), and one strategy for neuroprotective therapy for PD is to scavenge reactive species using a catalytic antioxidant. Previous studies in our laboratory revealed that pretreatment of lipophilic metalloporphyrins showed protective effects in a mouse PD model. In this study, we optimized the formulations of these metalloporphyrins to deliver them orally and tested their efficacy on disease outcomes in a second species after initiation of an insult (i.e., disease modification). In this study, a pharmaceutical formulation of two metalloporphyrin catalytic antioxidants, AEOL11207 and AEOL11114, was tested for oral drug delivery. Both compounds showed gastrointestinal absorption, achieved high plasma concentrations, and readily penetrated the blood-brain barrier after intravenous or oral delivery. AEOL11207 and AEOL11114 bioavailabilities were calculated to be 24% and 25%, respectively, at a dose of 10 mg/kg via the oral route. In addition, both compounds significantly attenuated 6-hydroxydopamine (6-OHDA)-induced neurotoxic damage, including dopamine depletion, cytokine production, and microglial activation in the striata; dopaminergic neuronal loss in the substantia nigra; oxidative/nitrative stress indices (glutathione disulfide and 3-nitrotyrosine) in the ventral midbrain; and rotation behavioral abnormality in rats. These results indicate that AEOL11207 and AEOL11114 are orally active metalloporphyrins and protect against 6-OHDA neurotoxicity 1–3 days postlesioning, suggesting disease-modifying properties and translational potential for PD.

SIGNIFICANCE STATEMENT

Two catalytic antioxidants showed gastrointestinal absorption, achieved high plasma concentrations, and readily penetrated the blood-brain barrier. Both compounds significantly attenuated dopamine depletion, cytokine production, microglial activation, dopaminergic neuronal loss, oxidative/nitrative stress indices, and behavioral abnormality in a Parkinson disease rat model. The results suggest that both metalloporphyrins possess disease-modifying properties that may be useful in treating Parkinson disease.

Introduction

The pathogenesis of dopaminergic neuronal death in the substantia nigra (SN) of patients with Parkinson disease (PD) is complex and remains to be fully elucidated. Current therapeutic approaches for PD are symptomatic and fall short of halting the disease progression or modifying outcomes leading to the need for identifying and investigating novel therapeutic targets and entities. Oxidative stress is thought to be a major mediator leading to dopaminergic neuron loss in both sporadic and genetic forms of PD (Zhang et al., 2000; Henchcliffe and Beal, 2008). Dopaminergic neurons in the SN are exposed to oxidative stress from several major sources, which include 1) dopamine (DA) auto-oxidation, enzymes such as monoamine oxidase, tyrosine hydroxylase, and mitochondrial aconitase, that release H_2O_2 under normal or oxidant stress conditions (Liang et al., 2007; Dias et al., 2013; Zhang et al., 2019). The emitted H_2O_2 can be further catalyzed into more toxic hydroxyl radicals (OH•) by adventitious reduced Fe^{2+} through the Fenton's reaction. DA can undergo non-enzymatic auto-oxidation reactions, resulting in the formation of superoxide ($O_2^{-\bullet}$) and H_2O_2 as well as reactive quinones (Graham, 1978). 2) Mitochondrial dysfunction, mitochondria complex I inhibition, which was found in the postmortem of SN (Schapira et al., 1990), and platelets (Krige et al., 1992) of patients with PD, is also an important source of $O_2^{-\bullet}$. Several

This study was supported by the Michael J. Fox Foundation Novel Approaches to Drug Discovery (NADD) Award 2012–2013 (M.P.).
Drs. Day and Patel are inventors on United States patents related to these metalloporphyrins.
[1]Current affiliation: Takeda Pharmaceuticals, San Diego, California.
[S] This article has supplemental material available at jpet.aspetjournals.org.

ABBREVIATIONS: AUC, area under the curve; BBB, blood-brain barrier; DA, dopamine; GSH, glutathione; GSSG, glutathione disulfide HPLC: High-performance liquid chromatography; H_2O_2 hydrogen peroxide IL-1β, interleukin-1β; IL-6, interleukin-6; IFN-γ, interferon-γ *Iba-1 ionized calcium adaptor molecule 1*; KC/GRO, keratinocyte chemoattractant/growth-related oncogene; MAPE, median absolute performance error; MPE, median performance error; MPTP, 1-methyl-4-phenyl-1,2,3,6-tetrahydropyridine; MSD, Meso Scale Discovery; NO, nitric oxide; 3-NT, 3-nitrotyrosine; $O_2^{-\bullet}$, superoxide; 6-OHDA, 6-hydroxydopamine; $ONOO^-$, peroxynitrite anion; PEG 400 poly (etylene glycol) 400 PD, Parkinson disease; PK, pharmacokinetic; SD, Sprague-Dawley; SN, substantia nigra; SNpc, substantia nigra pars compacta; $t_{1/2}$, terminal half-life; TH, tyrosine hydroxylase; TNF-α, tumor necrosis factor-α.

Downloaded from jpet.aspetjournals.org at ASPET Journals on April 19, 2024

gene mutations linked with PD, such as alpha-synuclein (α-syn), parkin, protein deglycase (DJ-1), and (PTEN-induced putative kinase 1) PINK1, initiate oxidative stress, leading to protein aggregation while simultaneously damaging mitochondrial dynamics, function, and integrity (Blesa et al., 2015). 3) Microglial activation, one important hallmark of PD, induces neuroinflammation and releases proinflammatory cytokines and nitric oxide (NO) (Beal, 2003). NO readily reacts with $O_2^{-\bullet}$ to form highly reactive peroxynitrite anions ($ONOO^-$). Collectively, these pathways suggest that oxidative stress is an important therapeutic target in PD, and targeting it with small-molecule antioxidant therapy could be a neuroprotective strategy for PD treatment (Zhou et al., 2008; Filograna et al., 2016).

Mesoporphyrin metalloporphyrins are synthetic small-molecule catalytic antioxidants with at least four distinct antioxidant properties due to their ability to scavenge $O_2^{-\bullet}$, H_2O_2, $ONOO^-$, and lipid peroxides (Day, 2004). Our laboratory has previously shown that lipophilic metalloporphyrins such as AEOL11207 and AEOL11114 protect against 1-methyl-4-phenyl-1,2,3,6-tetrahydropyridine (MPTP)-induced neurotoxicity in mouse models (Liang et al., 2007, 2017). The acute MPTP mouse model replicates many features of PD and is one of the classic models used to elucidate the pathogenesis of dopaminergic neuronal death. However, it typically induces DA neuronal death in just days or a week, necessitating pretreatment of therapeutic compounds, and is therefore inconsistent with the slow progression of clinical PD that may take several decades. Thus, it does not provide an ideal time window for studying neuroprotection and disease modification (Przedborski and Jackson-Lewis, 1998). To accelerate metalloporphyrin clinical development, it is necessary to test their efficacy in additional species and PD animal models. Additionally, rather than pretreatment paradigms, it is important to initiate their treatment after the insult to determine any translational potential and disease modification.

6-Hydroxydopamine (6-OHDA) is a hydroxylated analog of the natural neurotransmitter dopamine and neurotoxin (Blum et al., 2001). Intracerebral infusion of 6-OHDA induces significant DA depletion in the striata and massive dopaminergic neuron loss in the SN, which reproduces the most important biochemical and pathologic features of human PD, respectively (Uretsky and Iversen, 1970; Ungerstedt et al., 1974). The rat 6-OHDA model of PD was introduced more than 40 years ago, and despite numerous animal models developed for PD, it remains widely used because of the relatively low complexity and excellent reproducibility (Deumens et al., 2002). Intrastriatal infusion of 6-OHDA causes early DA depletion in the striatum, followed by a delayed, progressive dopaminergic neuronal loss in the SN and a substantially stable rotational behavioral response to apomorphine during the 4- to 8-week period, which provides a longer window to evaluate neuroprotective therapies (Sauer and Oertel, 1994; Przedborski et al., 1995; Blandini et al., 2007). Taken together, intrastriatal 6-OHDA is a relatively well accepted PD rat model for therapeutic testing. It offers a better strategy for examining innovative treatments designed to exert neuroprotection and disease modification. The goal of this study was to conduct pharmacokinetics (PK), including oral bioavailability, terminal half-lives ($t_{1/2}$), C_{max}, and blood-brain barrier (BBB) permeability, of AEOL11207 and AEOL11114 to guide a dosing regimen for assessing their efficacy for disease modification in an intrastriatal 6-OHDA rat model of parkinsonism.

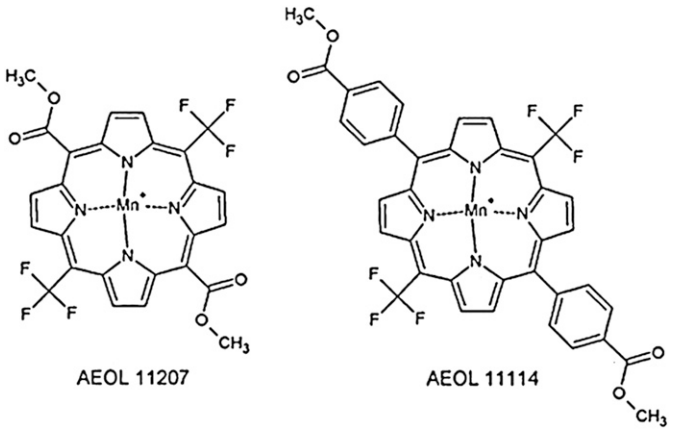

Fig. 1. Structures of metalloporphyrins. AEOL11114 molecular mass: 802.99. AEOL11207 molecular mass: 650.80.

Materials and Methods

Reagents

All reagents, including 6-OHDA hydrochloride, were purchased from Sigma-Aldrich (Sigma-Aldrich Corp., St. Louis, MO). AEOL11207 and AEOL11114 (see Fig. 1) were characterized as previously described (Liang et al., 2007, 2017).

Animals

Animal studies were carried out in accordance with the National Institutes of Health Guide for the Care and Use of Laboratory Animals (NIH Publications number 80-23). All procedures were approved by the Institutional Animal Care and Use Committee of the University of Colorado Anschutz Medical Campus. Male Sprague-Dawley (SD) rats (~300 g) purchased from Harlan Laboratories (Indianapolis, IN) were used for all experiments. After their arrival, rats were housed in groups on a 12-hour light/dark cycle and allowed ad libitum access to food and filtered water. All experiments were performed after 1 week of acclimatization of the rats.

Metalloporphyrins Pharmacokinetic Analysis

Metalloporphyrin Administration for PK Analysis. Male SD rats were treated with AEOL11207 or AEOL11114 (10 mg/kg) by tail intravenous injection with a 25-gauge needle or orally with a 5-inch-long standard rat's stomach tube. AEOL11207 or AEOL11114 was dissolved in 18% (v/v) PEG 400, 2% (v/v) benzyl alcohol, and 30% (v/v) propylene glycol. At 1, 6, 12, 24, 48, and 96 hours after metalloporphyrin administration, rats were deeply anesthetized with sodium pentobarbital (50 mg/kg, i.p.), and blood samples (~0.2 ml) were obtained by cardiac puncture with a 25-gauge needle. Rats were perfused transcardially with 80–100 ml saline to remove blood contamination in their brains, and brains were snap-frozen on dry ice. In some studies, blood samples were centrifuged at 13,000 rpm for 10 minutes, ~100 μl of plasma was collected, and both brain and plasma samples were stored at −80°C until use.

Measurement of Metalloporphyrin Levels. Metalloporphyrin levels were measured using an HPLC equipped with UV detector (Elite LaChrom System; Hitachi) and a YMC-Pack ODS-A column (4.6 × 150 mm, 3 μm, 120 Å; Waters, Milford, MA) as described previously (Kachadourian et al., 2002). The mobile phase contained 20 mM triethylamine and 20 mM trifluoroacetic acid (pH 2.7) and 70% acetonitrile with a flow rate of 1 ml/min. Proteins were extracted and precipitated from plasma and brain samples using 50%–75% methanol

Downloaded from jpet.aspetjournals.org at ASPET Journals on April 19, 2024

and 0.05 N perchloric acid followed by centrifugation at 16,000*g* for 20 minutes. An aliquot of the supernatant (10 μl) was injected into the HPLC with UV detector set at 450 nm for the AEOL11207 assay and 456 nm for theAEOL11114 assay; these wavelengths are close to the sort bands for each metalloporphyrin.

Metalloporphyrin PK Analysis and Modeling. Noncompartmental analysis of AEOL11207 and AEOL11114 plasma concentration was performed using Phoenix WinNonlin 8.1.0. (Certara USA, Inc., Princeton, NJ). To generate a model that could be used to simulate brain concentrations under different dosing schemes, a semi-physiologic pharmacokinetic model was generated. A compartmental model was used to describe the plasma concentration, which was coupled to a physiologic model for the brain to describe concentration-time data measured in the rat brain. Model fits and simulations were conducted with simulation, analysis and modeling II (SAAM II) version 2.3.1 (The Epsilon Group, Charlottesville, VA).

The model predictive capability was determined by calculating the median absolute performance error (MAPE%) and the median performance error (MPE%) for time-concentration curves and by comparison of calculated noncompartmental PK parameters for the actual data sets versus the physiologically based pharmacokinetic (PBPK) model simulations. The performance error (*PE*) calculation is shown in eq. 3 (Gustafsson et al., 1992).

$$PE = \frac{C_{measured} - C_{predicted}}{C_{predicted}} \bullet 100\% \quad (1)$$

MAPE%, a measure of prediction accuracy, was calculated as

$$MAPE\% = median(|PE_1|, |PE_2|, ...|PE_n|), \quad (2)$$

where n is the total number of samples for that tissue. *MPE%*, a measure of prediction bias, was calculated by

$$MPE\% = median(PE_1, PE_2, ...PE_n) \quad (3)$$

Metalloporphyrins' Effects on 6-OHDA Neurotoxicity

6-OHDA Model. 6-OHDA hydrochloride (free base) (20 μg) dissolved in 4 μl of 0.2% ascorbate in saline or 4 μl of 0.2% ascorbate in saline (sham) was infused at 0.5 μl/min using a motor-drive injector with a 26-gauge needle into the left striatum of male SD rats at the following coordinates (in millimeters with respect to bregma and dura): anterior-posterior (AP) −0.5, lateral (L) 2.5, and dorsal-ventral (DV) 4.5 (Paxinos and Watson, 1995). The 6-OHDA lesion model was validated in a preliminary experiment (see Supplemental Fig. 1).

Measurement of DA Levels. Striatal DA levels were measured using an HPLC (CoulArray system ESA model 5600; ESA, Boston, MA) equipped with an electrochemical detector (Liang and Patel, 2004). Briefly, rat striata were frozen in liquid nitrogen immediately after harvesting and sonicated in ice-cold 0.2 M perchloric acid (10% w/v), followed by centrifugation at 16,000*g* for 15 minutes at 4°C to precipitate proteins. An aliquot (20 μl) of the supernatant was separated by a column (3 μm, 100 × 4.6 mm; Waters) ideal for detection of catecholamines with an automatic sampler (ESA model 540), and the electrochemical detector potentials were set at 0/50/200/300 mV (vs. palladium). The mobile phase was composed of 100 mM citric acid, 2% methanol, 1 mM EDTA, and 5 mg/l sodium octyl sulfate (pH 3.0), and the flow rate was set at 0.6 ml/min.

Measurement of Redox Biomarkers. Glutathione (GSH), glutathione disulfide (GSSG), tyrosine, and 3-nitrotyrosine (3-NT) were assayed with an ESA 5600 CoulArray HPLC equipped with eight electrochemical cells following the company instruction (ESA application note 70–3993) as described in the literature (Beal et al., 1990) with additional modifications (Liang et al., 2007). The electrochemical cells were set at 400/450/500/570/630/690/810/860 mV (vs. palladium) potentials. An aliquot (20 μl) of the supernatant was separated on a TOSOHAAS (Montgomeryville, PA) reverse-phase octadecylsilyl (ODS) 80-TM C-18 analytical column (4.6 × 250 mm; 5-μm particle size). A two-component gradient elution system was used with component A of the mobile phase composed of 50 mM NaH_2PO_4 (pH 2.7) and component B composed of 50 mM NaH_2PO_4 and 50% methanol (pH 2.7). Mobile-phase flow rate was set at 0.8 ml/min. The initial gradient condition was 95% A and 5% B for 10 minutes, and the linear gradient was set to 70% A and 30% B from 10 to 30 minutes. The flow rate condition was retained at 70% A and 30% B from 30 to 40 minutes and back to 95% A and 5% B from 40 to 45 minutes, with an equilibration time running from 45 to 60 minutes. The levels of 3-NT were expressed as a ratio of 3-NT to tyrosine.

Tyrosine Hydroxylase Immunohistochemistry Staining and Stereological Cell Counting. Sections (40 μm) including the whole midbrain region were immunostained with 1:500 rabbit antibody/tyrosine hydroxylase (TH) (AB152; Chemicon, Temecula, CA) using the Avidin-Biotin Complex (ABC) method (ABC Elite Kit; Vector Laboratories, Burlingame, CA). Sections were counterstained with cresyl violet after TH staining. The number of TH-positive neurons at every fourth section was quantified with stereological analysis following previously described methods (West, 1999; Liang et al., 2007, 2017). The stereological method was used to determining the number of DA neurons using a computer-assisted image analysis system consisting of a Nikon Optiphot-2 80i microscope (Nikon, Inc., Melville, NY) equipped with a Motorized XYZ-Axis - Linear Compact (MC-XYZ-LC) (Applied Scientific Instrumentation, Eugene, OR) computer-controlled motorized stage. The substantia nigra pars compacta (SNpc) was delineated on each section at low magnification (4×), followed by systematic sampling at 60× magnification starting from a random start position using unbiased stereological analysis performed with the optical fractionator from StereoInvestigator (MicroBrightfield, Williston, VT). The number of TH-positive neurons in the ipsilateral site of SNpc of sham rats was expressed as 100%.

Microglial Activation Immunohistochemical Staining. The 20-μM thin brain sections including the whole striatum were immunostained with primary antibody anti–Iba-1 (ionized calcium adaptor molecule 1; Rabbit, Wako, Japan) and a Rhodamine Red conjugated goat anti-rabbit secondary antibody (1:100; Jackson Immuno Research, Inc.). Images were captured using a Nikon Eclipse TE2000-U microscope. Iba-1–positive signal of a given area was quantified with ImageJ software (National Institutes of Health, Bethesda, MD) in three sections, 100 μm apart, in the striatum of each animal. The average of the fluorescent relative density in the ipsilateral side of the striatum of sham rats was expressed as 100%.

Multiplex Proinflammatory Cytokine Measurement. Levels of tumor necrosis factor-α (TNF-α), interleukin-1β (IL-1β), interleukin-6 (IL-6), keratinocyte chemoattractant/growth-related oncogene (KC/GRO), and interferon-γ (IFN-γ) were measured using a rat multiplex

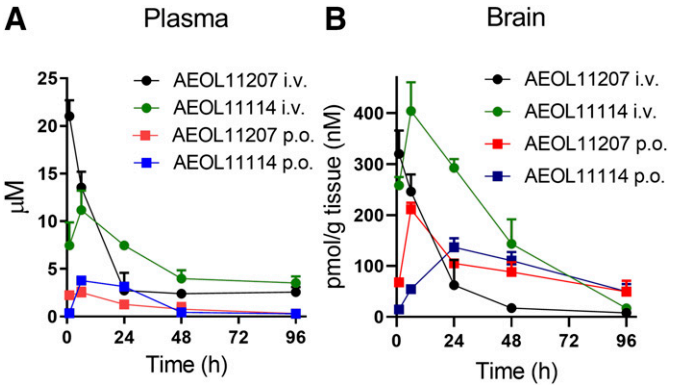

Fig. 2. The concentration of AEOL11207 or AEOL11114, dissolved in a new pharmaceutical formulation (18% PEG 400, 2% benzyl alcohol, and 30% propylene glycol), in the plasma (A) and brains (B) of rats 1, 6, 24, 48, and 96 hours after a single dose of AEOL11207 or AEOL11114 (10 mg/kg) by tail intravenous or per oral (p.o.) administration. Points represent means ± S.D. Each point is the average of three animals.

Downloaded from jpet.aspetjournals.org at ASPET Journals on April 19, 2024

TABLE 1
Summary of noncompartmental analysis results of metalloporphyrins

			F	$t_{1/2}^{a}$	C_{max}	AUC_{0-96}
			%	h	μM	μM × h
Plasma	AEOL11207	Intravenous			21.0	436
		By mouth	23	38	2.53	99
	AEOL11114	Intravenous			11.2	540
		By mouth	25	169	3.78	134
Brain	AEOL11207	Intravenous			0.32	15.0
		By mouth			0.21	9.3
	AEOL11114	Intravenous			0.40	19.2
		By mouth			0.14	8.7

F, bioavailability.
[a]The terminal half-lives in the plasma were estimated.

proinflammatory cytokine array kit (V-PLEX) from Meso Scale Discovery (MSD, Inc., Rockville, MD) according to the manufacturer's instructions and as described previously (McElroy et al., 2017; Liang et al., 2019). Briefly, striatal tissue was sonicated in 10% w/v (0.1 g tissue per milliliter) of a lysis buffer with protease and phosphatase inhibitors and centrifuged at 2000*g* for 5 minutes at 4°C. After a 1-hour period of blocking, an aliquot of 50 μl of supernatant or standards was loaded in duplicate and incubated at room temperature with shaking (700 rpm) for 2 hours. Standard curves were prepared with the supplied diluent from a range 0 pg/ml to 40,000 pg/ml. After washing three times with phosphate-buffered saline + 0.05% Tween 20, 25 μl of detection mixed antibodies was added and incubated at room temperature with shaking (700 rpm) for an additional 2 hours. After washing three times, the reading buffer was added, and the plate was read using MSD QuickPlex SQ 120 instrument (MSD, Inc.) by measuring the intensity of light emitted at 620 nm. The data analyses were performed with DISCOVERY WORKBENCH 4.0 software (MSD, Inc.) using curve-fit models.

Behavioral Testing. Apomorphine (0.5 mg/kg in 0.1% ascorbic acid, i.p.) was used to induce rotational activity in rats. The rotational behavior was measured using an automated rotameter consisting of a rotation bowl and a tether attached to the torso of the rat (San Diego Instruments, San Diego, CA) at 4 weeks postlesion as described previously (Ungerstedt and Arbuthnott, 1970). The number of complete turns performed by the animals was monitored by an automated recording system for 60 minutes.

Statistical Analysis

All data are expressed as means ± S.D. Statistical differences were analyzed by one-way ANOVA with Tukey-Kramer's post hoc tests. A P value less than 0.05 was considered statistically significant. All analyses were performed using Prism 8 software (Prism 8; GraphPad Software, San Diego, CA).

Results

Metalloporphyrin PK Analysis and Modeling to Optimize Dosing. PK parameters, including C_{max}, $t_{1/2}$, area under the curve (AUC), and oral bioavailability, were calculated by noncompartmental analysis from measured data (Fig. 2; Table 1). C_{max} of both AEOL11207 and AEOL11114 achieved high plasma and brain concentrations after oral administration, suggesting that the compounds were well absorbed by the gastrointestinal tract. Relatively high AUC in brain indicated the compounds' ability to penetrate the BBB. A single bolus dose of 10 mg/kg resulted in estimated percentages of oral bioavailabilities calculated by AUC oral/AUC intravenous of AEOL11207 and AEOL11114 to be 23% and 25%, respectively. The $t_{1/2}$ for the compounds could only be estimated because of the lack of a consistent decrease in drug concentration over an adequate sampling time. The estimated $t_{1/2}$ was 38 hours for AEOL11207 and 170 hours for AEOL11114 (Table 1).

A semiphysiologic PK model was generated to describe the oral plasma and brain concentration-time data for both AEOL11207 and AEOL11114 (Fig. 3). Oral concentration-time data of both compounds was fit to a two-compartment model with first-order absorption (Fig. 3). The model predictive capability, calculated with percentages of MAPE and MPE, indicated that the models for both AEOL11207 and AEOL11114 describe the plasma and brain data reasonably well, although they overpredicted measured data slightly (Table 2). The model was used to simulate different dosing regimens that could yield a plasma concentration of ~1 μM and brain concentrations in the range of 100–150 nM, which were previously found to be protective in the MPTP mouse model (Liang et al., 2007, 2017). The simulations suggest that both compounds should achieve the desired plasma and brain concentrations when administered orally at either 5 mg/kg daily or 10 mg/kg every other day (Fig. 4).

Metalloporphyrins Protect against 6-OHDA–Induced Oxidative/Nitrative Stress. GSH and its oxidized disulfide form, GSSG, are widely used as biomarkers of the cellular or tissue redox status (Valko et al., 2007). 3-NT, formed in proteins after the reaction of tyrosine residues with $ONOO^-$, is an indicator of protein nitration, a post-translational modification capable of inducing protein dysfunction (Sawa et al., 2000). To determine a therapeutic time window, we first established the time course of GSH, GSSG, and 3-NT after 6-OHDA treatment. Given the high millimolar tissue levels of

Downloaded from jpet.aspetjournals.org at ASPET Journals on April 19, 2024

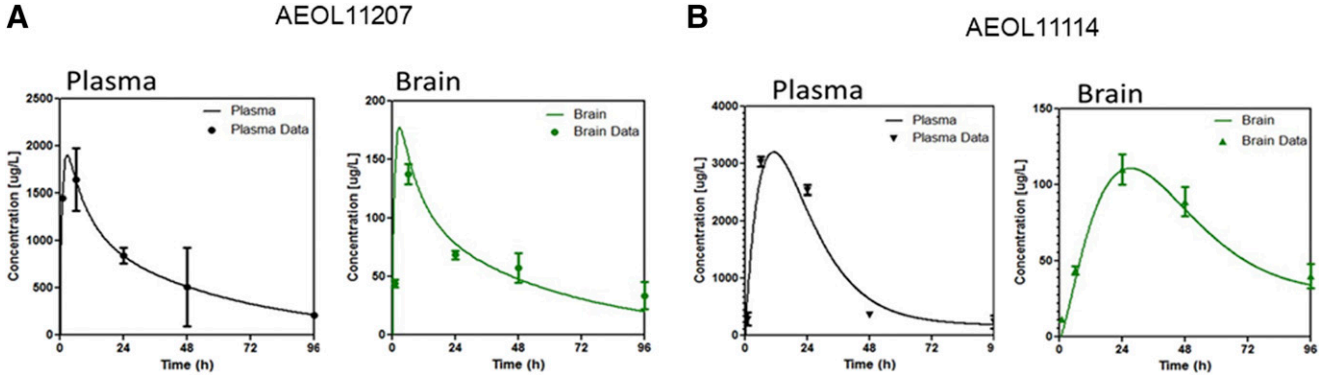

Fig. 3. A semiphysiologic pharmacokinetic model was fit to AEOL11207 (A) and AEOL11114 (B) plasma and brain oral concentration-time data.

TABLE 2
Model predictive values
For the detailed calculation protocol, see *Materials and Methods* section.

	MAPE		MPE	
	Plasma	Brain	Plasma	Brain
		%		
AEOL11207	7.6	21.9	−2.8	−7.7
AEOL11114	26.9	17.7	10.2	17.7

GSH, it was not significantly altered by 6-OHDA treatment. However, GSSG and 3-NT were significantly increased to 190%–200% in the lesioned side of ventral midbrain, with the highest levels being reached at 14 and 28 days after 6-OHDA infusion compared with those of the sham, respectively (Fig. 5A). We next assessed the dose dependence and dosing frequency of AEOL11207 and AEOL11114 capable of preventing 6-OHDA–induced oxidative/nitrative stress. When AEOL11207 and AEOL11114 were orally administered at a dose of 10 mg/kg every other day starting at 1 day post–6-OHDA infusion, 6-OHDA–induced oxidative/nitrative stress was substantially inhibited 14 days post–6-OHDA administration (Fig. 5B). Given the oxidative/nitrative stress biomarkers and PK results, a dosing regimen for both AEOL11207 and AEOL11114 of 10 mg/kg via the oral route every other day was selected for its ability to alter 6-OHDA–induced DA depletion and TH cell death.

Metalloporphyrins Protect against 6-OHDA–Induced Striatal DA Depletion. Measurement of striatal DA levels revealed that, 4 weeks after intrastriatal vehicle infusion (sham), DA levels were 67.98 ± 4.45 nmol/g tissue (mean ± S.D., n = 6) compared with DA levels in striata of naïve animals (DA: 66.58 ± 8.19 nmol/g tissue; mean ± S.D.; n = 4; see Supplemental Fig. 1), suggesting that the sham treatment did not cause DA depletion, consistent with previous studies (Deumens et al., 2002). Compared with sham rats, striatal DA levels were decreased by 65%–70% in the lesioned side of the striata 4 weeks after 6-OHDA infusion. Compared with vehicle treatment in sham rats, treatment with AEOL11207 and AEOL11114 (initiated 1 day postlesion for 4 weeks) decreased striatal DA levels by 34.7% and 40.3%, respectively. This suggested that the compounds exert a protective effect on dopaminergic terminals in the 6-OHDA model 1 day postlesion. However, no statistically significant protective effect was found when the AEOL11207 or AEOL11114 regimen was initiated 3 days postlesion as compared with that of the 6-OHDA with vehicle group (Fig. 6).

Metalloporphyrins Protect against 6-OHDA–Induced DA Neuronal Loss. The dopaminergic neurons (TH-positive neurons) in the SNpc were significantly decreased 40%–45% in

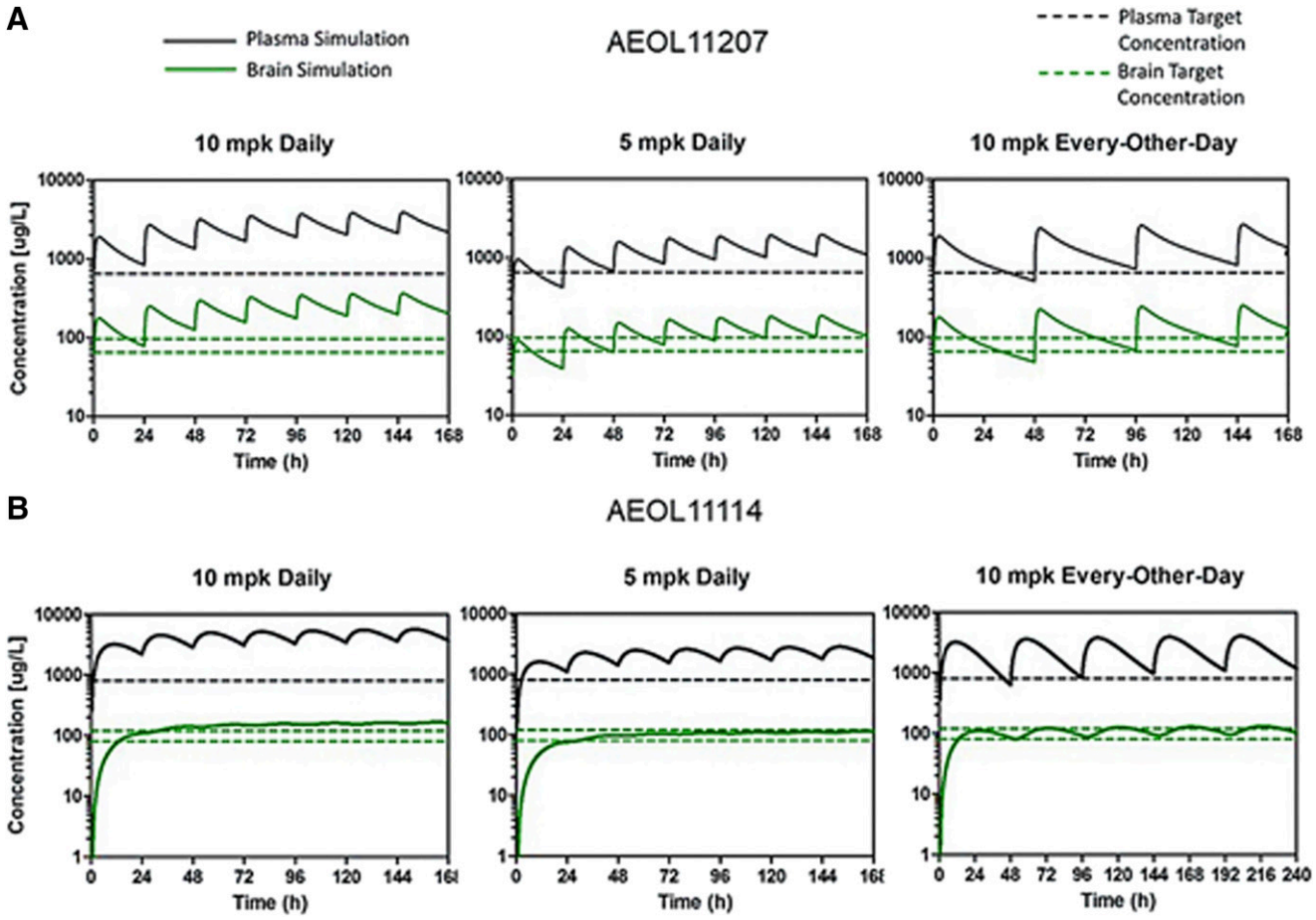

Fig. 4. Dosing scheme simulations for AEOL11207 (A) and AEOL11114 (B). The semiphysiologic pharmacokinetic model was used to simulate plasma and brain concentration-time data under different dosing regimens. Simulations were used to establish a dose and dosing schedule of AEOL11207 that would achieve a plasma minimum concentration (C_{min})of ~1 μM and brain C_{min} in the range of 100–150 nM and were used to establish a dose and dosing schedule of AEOL11114 that would achieve a plasma C_{min} of ~1 μM (803 μg/l) and brain C_{min} in the range of 100–150 nM (80–120 μg/l). mg/kg (mpk)

Downloaded from jpet.aspetjournals.org at ASPET Journals on April 19, 2024

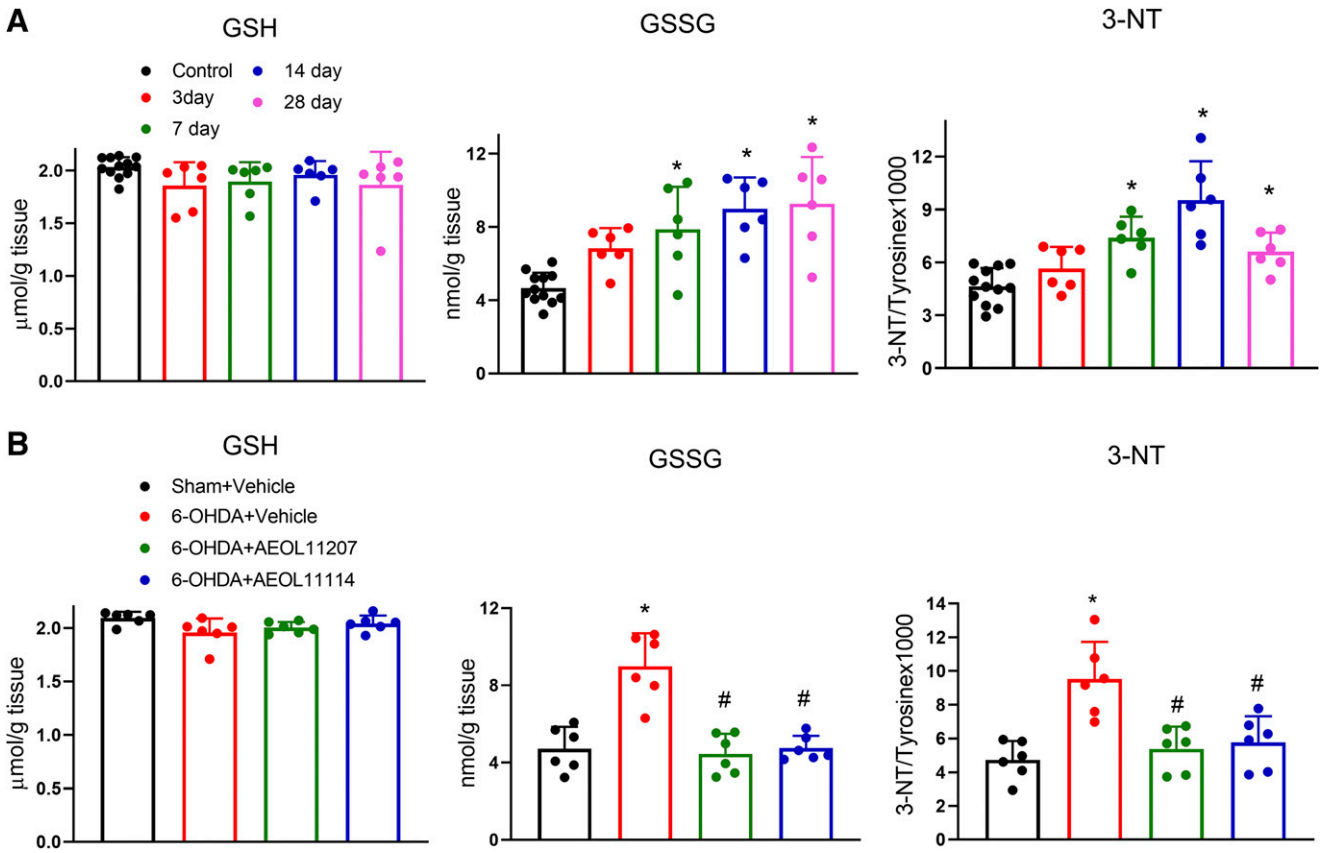

Fig. 5. (A) GSH, GSSG, and 3-NT in the ipsilateral site of the ventral midbrain of rats 3, 7, 14, and 28 days post–6-OHDA (20 µg) in 4 µl saline solution containing 0.02% ascorbic acid or the same volume of 0.02% ascorbic acid in saline (sham) intrastriatal infusion. Bars represent means + S.D. $^{*}P < 0.01$ vs. sham, one-way ANOVA test with Tukey-Kramer's post hoc tests: GSH [F (4–31) = 1.36, $P = 0.269$]; GSSG [F (4–31) = 10.96, $P < 0.001$]; 3-NT [F (4–31) = 14.39, $P < 0.001$]; n = 6–12 rats per group. (B) GSH, GSSG, and 3-NT in the ipsilateral site of the ventral midbrain of rats 14 days with vehicle (18% PEG 400, 2% benzyl alcohol, and 30% propylene glycol), AEOL11207, or AEOL11114 (10 mg/kg, by mouth) every other day starting at 1 day post–6-OHDA intrastriatal infusion or sham. Bars represent means + S.D. $^{*}P < 0.01$ vs. sham + vehicle, $^{\#}P < 0.05$ vs. 6-OHDA + vehicle, one-way ANOVA with Tukey-Kramer's post hoc tests: GSH [F (3–20) = 2.79, $P = 0.067$]; GSSG [F (3–20) = 19.82, $P < 0.0001$]; 3-NT [F (3–20) = 10.86, $P = 0.0002$]; n = 6 rats per group.

the lesioned side compared with those of the sham animals. 6-OHDA–induced dopaminergic neuronal loss in the SNpc were decreased only 5%–10% compared with those of sham animals when treatment with AEOL11207 and AEOL11114 starting on day 1 or 3 postlesion. (Fig. 7). These results suggest a significant neuroprotective effect of AEOL11207 and AEOL11114 against 6-OHDA toxicity on dopaminergic neurons.

Metalloporphyrins Protect against 6-OHDA–Induced Microglial Activation. To determine whether AEOLs prevent 6-OHDA–induced inflammatory effects, immunohistochemistry staining performed with Iba-1, a marker of microglial activation (Kanazawa et al., 2002), was investigated. An increase in average fluorescence density of Iba-1 in the 6-OHDA lesion side of the striata began 3 days and reached ~320% 14 days post–6-OHDA infusion compared with the sham group. The average fluorescence density increased 240% and 229% after 10 mg/kg AEOL11207 and AEOL11114 administered by mouth every other day starting 1 day postlesion compared with that of the sham group, respectively. Relative to the vehicle, AEOL11207 or AEOL11114 treatment attenuated 6-OHDA–induced Iba-1 fluorescence density by 37.2% and 42.1%, respectively (Fig. 8).

Metalloporphyrins Protect against 6-OHDA–Induced Alterations in Cytokine Production. IL-1β, IL-6, TNF-α, and KC/GRO (but not IFN-γ) levels were significantly elevated in the striata of the rats 3 and 5 days post–6-OHDA infusion (Table 3). IL-1β, IL-6, TNF-α, and KC/GRO levels were significantly increased by 1.7-, 61-, 34-, and 106-fold in the striata 5 days post–6-OHDA infusion compared with sham,

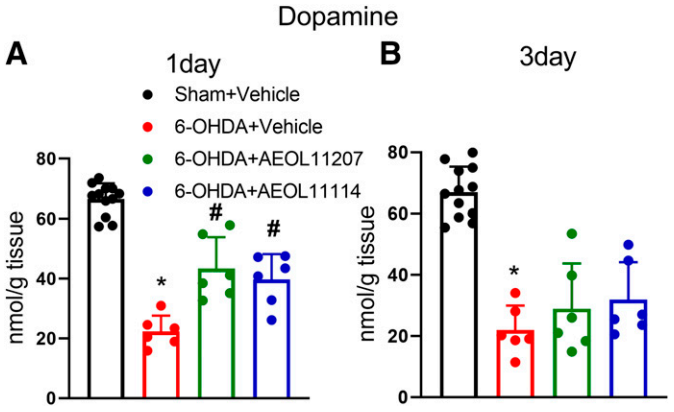

Fig. 6. Dopamine levels in the ipsilateral site of the striata of rats at 4 weeks with vehicle, AEOL11207, or AEOL11114 (10 mg/kg, by mouth) every other day starting at 1 day (A) or 3 days (B) post–6-OHDA intrastriatal infusion or sham. Bars represent means + S.D. $^{*}P < 0.01$ vs. sham + vehicle, $^{\#}P < 0.01$ vs. 6-OHDA + vehicle, one-way ANOVA with Tukey-Kramer's post hoc tests: 1 day [F (3–24) = 42.41, $P < 0.0001$]; 3 days [F (3–26) = 31.51, $P < 0.0001$]; n = 6–12 rats per group.

Downloaded from jpet.aspetjournals.org at ASPET Journals on April 19, 2024

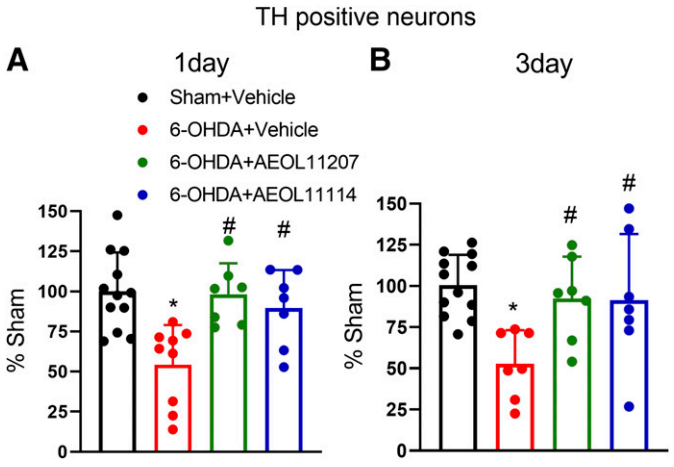

Fig. 7. Percentage of dopaminergic neurons (TH-positive neurons) in the ipsilateral site of the SNpc of rats at 4 weeks with vehicle, AEOL11207, or AEOL11114 (10 mg/kg, by mouth) every other day starting at 1 day (A) or 3 days (B) post–6-OHDA (20 μg) intrastriatal infusion or sham. Stereological neuronal counts were performed using unbiased stereological analysis. The number of TH-positive neurons in the ipsilateral site of SNpc with sham treatment rats as 100%. Bars represent means + S.D. $^{*}P < 0.01$ vs. sham + vehicle, $^{\#}P < 0.05$ vs. 6-OHDA + vehicle, one-way ANOVA with Tukey-Kramer's post hoc tests: 1 day [F (3–31) = 7.164, $P = 0.0006$]; 3 days [F (3–29) = 5.246, $P = 0.0051$]; n = 6–12 rats per group.

respectively. Given the robust increase in the majority of proinflammatory cytokines 5 days post–6-OHDA, this time point was selected to test the ability of metalloporphyrins to alter their production. Compared with vehicle treatment, AEOL11207 and AEOL11114 (initiated day 1 post–6-OHDA infusion) for a period of 5 days, attenuated IL-1β, IL-6, TNF-α, and KC/GRO levels in the striata by 40%, 73.5%, 72.4%, and 56.3%, respectively (Fig. 9). Together with their ability to attenuate microglial activation (assessed by Iba-1 staining), this suggests that these metalloporphyrins exert an anti-inflammatory effect in the 6-OHDA model.

Metalloporphyrins Protect against 6-OHDA–Induced Behavioral Abnormality. Apomorphine-induced rotational behavior was measured as another indicator of metalloporphyrins' neuroprotection. 6-OHDA–lesioned rats were challenged with apomorphine (0.5 mg/kg, i.p.) after 4 weeks, and the number of completed rotations was observed and recorded. 6-OHDA produced approximately 240–250 turns during a total of 60 minutes, indicating that lesioning was significant. Rats that received a vehicle infusion (sham) did not display any significant rotational behavior upon apomorphine challenge. 6-OHDA–induced increases in the number of rotations were significantly attenuated by 57.1% and 53.5% after AEOL11207 or AEOL11114, respectively, when administered at 1 day; however, no statistically significant attenuation was observed when the compounds were started 3 days postlesion as compared with the 6-OHDA with vehicle group (Fig. 10).

Discussion

In this study, we optimized two metalloporphyrins for favorable oral bioavailability, BBB permeability, and in vivo efficacy in a rat 6-OHDA model of PD. Using this dosing paradigm, we demonstrated that initiation of treatment with metalloporphyrins 1 or 3 days after the insult resulted in inhibition of dopamine depletion, neuroinflammation (increased cytokine levels and microglial activation in the striata), dopaminergic neuronal loss in the SNpc, oxidative/nitrative stress indices (GSSG and 3-NT formation) in the ventral midbrain, and rotation behavioral abnormality 4 weeks after intrastriatal 6-OHDA infusion in rats. Attenuation of dopaminergic neuronal loss (1 and 3 days) as well as behavioral

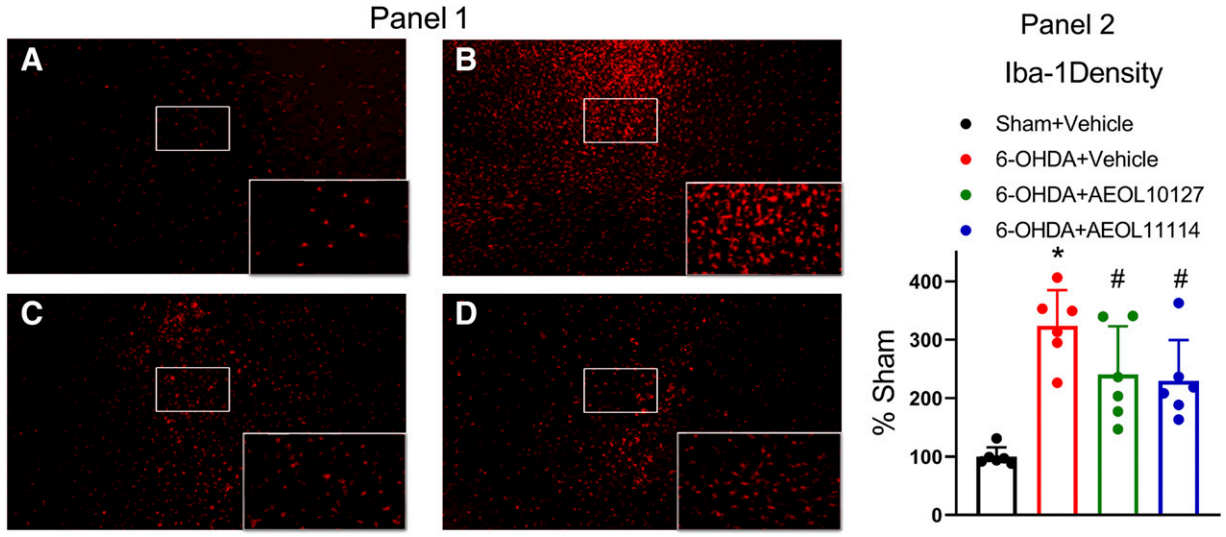

Fig. 8. (Panel 1) Representative microglial activation (Iba-1 staining) images in the ipsilateral site of the striata of rats 14 days after sham with vehicle (A) or 6-OHDA with vehicle (B), AEOL11207 (C), or AEOL11114 (D) (10 mg/kg, by mouth) every other day starting 1 day post–6-OHDA intrastriatal infusion or sham. The insets on the lower right corner of each picture are the enlarged image from the white rectangle. (Panel 2) Quantitative analysis of microglial activation fluorescence density in the ipsilateral site of the striata of rats 14 days with vehicle, AEOL11207, or AEOL11114 (10 mg/kg, by mouth) every other day starting 1 day post–6-OHDA intrastriatal infusion or sham. The microglial activation fluorescence density in each given area of striata was estimated with ImageJ. The fluorescence density average in the ipsilateral site of the striata with sham treatment rats as 100%. Bars represent means + S.D. $^{*}P < 0.01$ vs. sham + vehicle, $^{\#}P < 0.05$ vs. 6-OHDA + vehicle, one-way ANOVA with Tukey-Kramer's post hoc tests: 1 day [F (3–20) = 13.08, $P < 0.0001$]; n = 6 rats per group.

Downloaded from jpet.aspetjournals.org at ASPET Journals on April 19, 2024

TABLE 3

The levels of cytokines post–6-OHDA

Cytokine levels in the rat striatum 3 or 5 days post 6-OHDA infusion. Data are expressed as picograms per gram tissue (units) and depicted as means ± S.D.

	Sham	3 Days Post–6-OHDA	5 Days Post–6-OHDA
IL-1β	441 ± 130	748 ± 205*	746 ± 154*
IL-6	2177 ± 1464	90,409 ± 76,065*	135,621 ± 76,065*
TNF-α	48 ± 32	1802 ± 1231*	1661 ± 761*
KC/GRO	404 ± 134	33,575 ± 20,989*	43,222 ± 25,051*
IFN-γ	123 ± 83	114 ± 11	131 ± 94

*$P < 0.01$ vs. sham, one-way ANOVA with Tukey-Kramer's post hoc tests; $N = 4–6$.

deficits (1 day) postlesion with AEOL11207 and AEOL11114 suggests that both metalloporphyrins have translational potential and disease-modifying effects.

In this study, AEOL11207 and AEOL11114 were found to have good gastrointestinal absorption, oral bioavailability, BBB access, and extended plasma concentrations in rats. The pharmacokinetic analysis results from this study indicate that both compounds achieved a brain C_{max} in the range of 100–150 nM with a relatively low dose of drug (5 mg/kg every day or 10 mg/kg every other day via oral administration). Our previous studies have shown that 100–150 nM levels of AEOL11207 and AEOL11114 are protective against indices of neurotoxicity, including DA depletion in the striata, dopaminergic neuronal loss in the SNpc, and oxidative/nitrative stress (GSSG and 3-nitrotyrosine formation) in the ventral midbrain of MPTP-treated mice (Liang et al., 2007, 2017). By using the 6-OHDA model, we were able to demonstrate disease-modifying effects of these compounds in a second species and animal model of PD with similar concentrations of drug levels being achieved in the brain. Furthermore, the new formulation of the compounds, combined with the use of the 6-OHDA lesion model, revealed additional advantages to these compounds that were not present in our earlier work. First, the compounds were shown to be protective even when administered after the initial neurologic insult. In contrast, the compounds had to be administered prior to MPTP injury to achieve similar levels of protection in the MPTP mouse model (Liang et al., 2007, 2017). Secondly, a new formulation was selected that enables the oral route of administration and provides a relatively longer duration of drug action. This study shows that the rats were able to tolerate doses of the metalloporphyrins with this formulation. The maximum tolerated dose was about 60 mg/kg, which is higher than the dosing required for in vivo efficacy (5 mg/kg every day or 10 mg/kg every other day via oral route). In our previous work, the compounds were dissolved in 1% or 5% DMSO solution (Liang et al., 2007, 2017), which could be toxic to patients with PD over the course of long-term therapy.

Oxidative damage to dopaminergic neurons in the SNpc is considered to be one of the major pathogenic factors leading to neurodegeneration and motor disturbances in PD (Jenner, 2003). 6-OHDA is a hydroxylated analog of DA, which is actively transported into dopaminergic neurons via a dopamine transporter on the nerve terminals. It then selectively kills dopaminergic neurons via auto-oxidization to generate quinones, $O_2^{-\bullet}$, H_2O_2, and lipid peroxyl radicals (Cohen and Heikkila, 1974; Sachs and Jonsson, 1975). 6-OHDA treatment has been shown to deplete striatal GSH levels (Perumal et al., 1992) and increase the levels of malondialdehyde (Kumar et al., 1995), which further supports the role of oxidative stress in 6-OHDA toxicity. Previously, we have shown several key antioxidant properties of AEOL11207 and AEOL11114 based on their abilities to scavenge H_2O_2, $O_2^{-\bullet}$, and lipid peroxides (Liang et al., 2007, 2017; Castello et al., 2008), which likely underlie their protective effects against 6-OHDA neurotoxicity. Metalloporphyrins are a class of synthetic catalytic antioxidants that overcome many limitations of natural superoxide dismutase/catalase enzymes, such as large size, short circulation half-life, and antigenicity. These compounds act stoichiometrically and are much more potent than dietary antioxidants, such as ascorbate (vitamin C) and α-tocopherol (vitamin E) (Patel, 2016). This result further supports antioxidant therapy as a modality in preventing and combating aggressive dopaminergic neuronal degeneration in vivo.

Massive microglial activation has been observed in the progressive dopaminergic degenerative processes associated with PD autopsy specimens (Croisier et al., 2005) and animal models, including MPTP, 6-OHDA, rotenone, and paraquat (Yokoyama et al., 2011). Increased microglial activation has also been detected in both SN and striatum in the 6-OHDA model (He et al., 2001; Depino et al., 2003). Furthermore, a significant decrease in dopaminergic neuronal loss parallels a progressive increase in microglial activation over time

Downloaded from jpet.aspetjournals.org at ASPET Journals on April 19, 2024

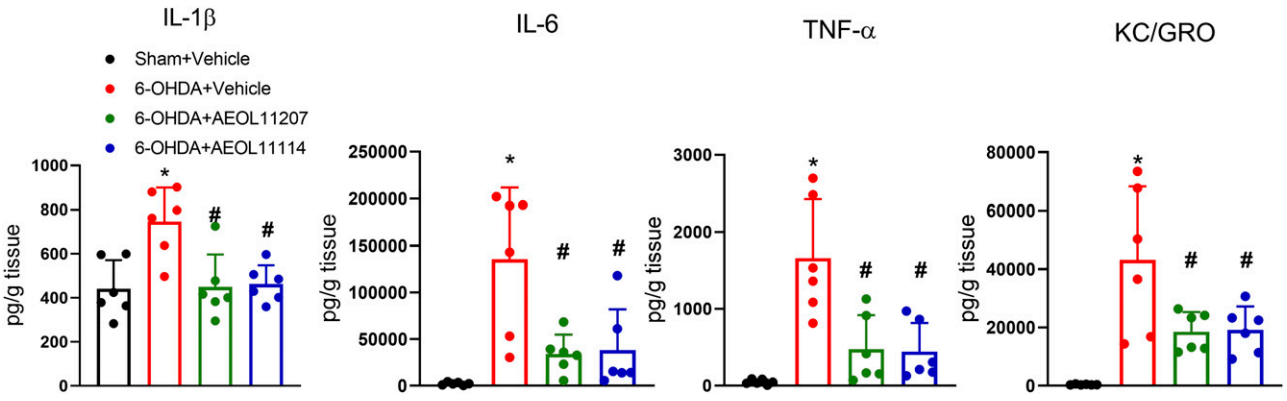

Fig. 9. IL-1β, IL-6, TNF-α, and KC/GRO levels in the striata injected with 6-OHDA 5 days after vehicle, AEOL11207, or AEOL11114 (10 mg/kg, by mouth) dosed every other day starting at 1 day post–6-OHDA intrastriatal infusion or sham. Bars represent means + S.D. *$P < 0.01$ vs. sham + vehicle, #$P < 0.01$ vs. 6-OHDA + vehicle, one-way ANOVA with Tukey-Kramer's post hoc tests: IL-1β [F (3–20) = 7.531, $P = 0.0015$]; IL-6 [F (3–20) = 9.820, $P = 0.0003$]; TNF-α [F (3–20) = 12.72, $P < 0.0001$]; KC/GRO [F (3–26) = 10.04, $P = 0.0003$]; $n = 6$ rats per group.

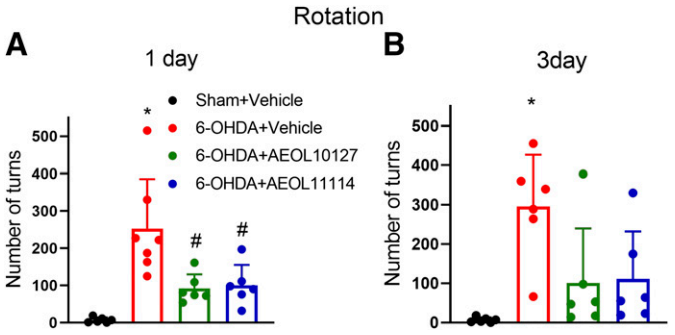

Fig. 10. The rotation behavior of rats 4 weeks with vehicle, AEOL11207, or AEOL11114 (10 mg/kg, by mouth) every other day starting at 1 day (A) or 3 days (B) post–6-OHDA (20 μg) intrastriatal infusion or sham. Rats were tested with systemic apomorphine administration (0.5 mg/kg in 0.1% ascorbic acid, i.p.). The number of turns was recorded by an automated recording system for 60 minutes. Bars represent means + S.D. $^{*}P < 0.01$ vs. sham + vehicle, $^{\#}P < 0.05$ vs. 6-OHDA + vehicle, one-way ANOVA with Tukey-Kramer's post hoc tests: 1 day [F (3–21) = 7.693, P = 0.0012]; 3 days [F (3–21) = 3.961, P = 0.0220]; n = 6 to 7 rats.

after 6-OHDA injection in rats monitored with positron emission tomography imaging (Cicchetti et al., 2002). Studies have shown that microglial activation plays a major role in DA neuronal degeneration through the release of large amounts of cytotoxic molecules, including a variety of proinflammatory cytokines and reactive oxygen species (Phani et al., 2012). Proinflammatory cytokines are also mediators of apoptosis, which plays an important role in dopaminergic neuronal death in patients with PD (Nagatsu and Sawada, 2005; Sawada et al., 2006). Therefore, inhibiting aberrant neuroinflammation and microglial activation has been a recognized strategy to preserve and protect dopaminergic neurons (Wu et al., 2002). Prior studies have demonstrated elevations in several key proinflammatory cytokines, including TNF-α, IL-1β, and IL-6, in the cerebrospinal fluid and the striata of patients with PD (Mogi et al., 1994a,b; Blum-Degen et al., 1995; Müller et al., 1998). Furthermore, released cytokines were accompanied by NO production, which was sensitive to attenuation, by NO synthase inhibition in primary mixed neuronal/glial cell cultures (Chao et al., 1996; Hu et al., 1997). Our results indicate a large elevation in several proinflammatory cytokines together with microglial activation, which were both significantly attenuated by metalloporphyrins, likely because of their ability to exert an antioxidant effect. It is consistent with the possible mechanism(s) of another metalloporphyrin, AEOL10150, protecting against seizure-induced oxidative/nitrative stress, microglial activation, and proinflammatory cytokine release (McElroy et al., 2017; Liang et al., 2019).

In summary, two glyoxylate metalloporphyrin catalytic antioxidants, AEOL11207 and AEOL11114, were identified as having significant ability to protect against 6-OHDA–induced neurotoxic damage in the PD rat model that is consistent with the previous results in the MPTP mouse PD model (Liang et al., 2017). Both compounds are orally active, readily penetrate the BBB, and may be useful for chronic neurologic diseases such as PD.

Authorship Contributions

Participated in research design: Liang, Day, Patel.
Conducted experiments: Liang, Fulton, Pearson-Smith.
Contributed new reagents or analytic tools: Bradshaw-Pierce, Day.
Performed data analysis: Liang, Bradshaw-Pierce, Day.
Wrote or contributed to the writing of the manuscript: Liang, Bradshaw-Pierce, Pearson-Smith, Day, Patel.

References

Beal MF (2003) Mitochondria, oxidative damage, and inflammation in Parkinson's disease. *Ann N Y Acad Sci* **991**:120–131.
Beal MF, Matson WR, Swartz KJ, Gamache PH, and Bird ED (1990) Kynurenine pathway measurements in Huntington's disease striatum: evidence for reduced formation of kynurenic acid. *J Neurochem* **55**:1327–1339.
Blandini F, Levandis G, Bazzini E, Nappi G, and Armentero MT (2007) Time-course of nigrostriatal damage, basal ganglia metabolic changes and behavioural alterations following intrastriatal injection of 6-hydroxydopamine in the rat: new clues from an old model. *Eur J Neurosci* **25**:397–405.
Blesa J, Trigo-Damas I, Quiroga-Varela A, and Jackson-Lewis VR (2015) Oxidative stress and Parkinson's disease. *Front Neuroanat* **9**:91.
Blum D, Torch S, Lambeng N, Nissou M, Benabid AL, Sadoul R, and Verna JM (2001) Molecular pathways involved in the neurotoxicity of 6-OHDA, dopamine and MPTP: contribution to the apoptotic theory in Parkinson's disease. *Prog Neurobiol* **65**:135–172.
Blum-Degen D, Müller T, Kuhn W, Gerlach M, Przuntek H, and Riederer P (1995) Interleukin-1 beta and interleukin-6 are elevated in the cerebrospinal fluid of Alzheimer's and de novo Parkinson's disease patients. *Neurosci Lett* **202**:17–20.
Castello PR, Drechsel DA, Day BJ, and Patel M (2008) Inhibition of mitochondrial hydrogen peroxide production by lipophilic metalloporphyrins. *J Pharmacol Exp Ther* **324**:970–976.
Chao CC, Hu S, Sheng WS, Bu D, Bukrinsky MI, and Peterson PK (1996) Cytokine-stimulated astrocytes damage human neurons via a nitric oxide mechanism. *Glia* **16**:276–284.
Cicchetti F, Brownell AL, Williams K, Chen YI, Livni E, and Isacson O (2002) Neuroinflammation of the nigrostriatal pathway during progressive 6-OHDA dopamine degeneration in rats monitored by immunohistochemistry and PET imaging. *Eur J Neurosci* **15**:991–998.
Cohen G and Heikkila RE (1974) The generation of hydrogen peroxide, superoxide radical, and hydroxyl radical by 6-hydroxydopamine, dialuric acid, and related cytotoxic agents. *J Biol Chem* **249**:2447–2452.
Croisier E, Moran LB, Dexter DT, Pearce RK, and Graeber MB (2005) Microglial inflammation in the parkinsonian substantia nigra: relationship to alpha-synuclein deposition. *J Neuroinflammation* **2**:14.
Day BJ (2004) Catalytic antioxidants: a radical approach to new therapeutics. *Drug Discov Today* **9**:557–566.
Depino AM, Earl C, Kaczmarczyk E, Ferrari C, Besedovsky H, del Rey A, Pitossi FJ, and Oertel WH (2003) Microglial activation with atypical proinflammatory cytokine expression in a rat model of Parkinson's disease. *Eur J Neurosci* **18**: 2731–2742.
Deumens R, Blokland A, and Prickaerts J (2002) Modeling Parkinson's disease in rats: an evaluation of 6-OHDA lesions of the nigrostriatal pathway. *Exp Neurol* **175**:303–317.
Dias V, Junn E, and Mouradian MM (2013) The role of oxidative stress in Parkinson's disease. *J Parkinsons Dis* **3**:461–491.
Filograna R, Godena VK, Sanchez-Martinez A, Ferrari E, Casella L, Beltramini M, Bubacco L, Whitworth AJ, and Bisaglia M (2016) Superoxide Dismutase (SOD)-mimetic M40403 is protective in cell and fly models of paraquat toxicity: implications for Parkinson disease. *J Biol Chem* **291**:9257–9267.
Graham DG (1978) Oxidative pathways for catecholamines in the genesis of neuromelanin and cytotoxic quinones. *Mol Pharmacol* **14**:633–643.
Gustafsson LL, Ebling WF, Osaki E, Harapat S, Stanski DR, and Shafer SL (1992) Plasma concentration clamping in the rat using a computer-controlled infusion pump. *Pharm Res* **9**:800–807.
He Y, Appel S, and Le W (2001) Minocycline inhibits microglial activation and protects nigral cells after 6-hydroxydopamine injection into mouse striatum. *Brain Res* **909**:187–193.
Henchcliffe C and Beal MF (2008) Mitochondrial biology and oxidative stress in Parkinson disease pathogenesis. *Nat Clin Pract Neurol* **4**:600–609.
Hu S, Peterson PK, and Chao CC (1997) Cytokine-mediated neuronal apoptosis. *Neurochem Int* **30**:427–431.
Jenner P (2003) Oxidative stress in Parkinson's disease. *Ann Neurol* **53** (Suppl 3): S26–S36; discussion S36–S38.
Kachadourian R, Menzeleev R, Agha B, Bocckino SB, and Day BJ (2002) High-performance liquid chromatography with spectrophotometric and electrochemical detection of a series of manganese(III) cationic porphyrins. *J Chromatogr B Analyt Technol Biomed Life Sci* **767**:61–67.
Kanazawa H, Ohsawa K, Sasaki Y, Kohsaka S, and Imai Y (2002) Macrophage/microglia-specific protein Iba1 enhances membrane ruffling and Rac activation via phospholipase C-gamma -dependent pathway. *J Biol Chem* **277**:20026–20032.
Krige D, Carroll MT, Cooper JM, Marsden CD, and Schapira AH; The Royal Kings and Queens Parkinson Disease Research Group (1992) Platelet mitochondrial function in Parkinson's disease. *Ann Neurol* **32**:782–788.
Kumar R, Agarwal AK, and Seth PK (1995) Free radical-generated neurotoxicity of 6-hydroxydopamine. *J Neurochem* **64**:1703–1707.
Liang LP, Huang J, Fulton R, Day BJ, and Patel M (2007) An orally active catalytic metalloporphyrin protects against 1-methyl-4-phenyl-1,2,3,6-tetrahydropyridine neurotoxicity in vivo. *J Neurosci* **27**:4326–4333.
Liang LP, Huang J, Fulton R, Pearson-Smith JN, Day BJ, and Patel M (2017) Preclinical therapeutic development of a series of metalloporphyrins for Parkinson's disease. *Toxicol Appl Pharmacol* **326**:34–42.

Downloaded from jpet.aspetjournals.org at ASPET Journals on April 19, 2024

Liang LP and Patel M (2004) Iron-sulfur enzyme mediated mitochondrial superoxide toxicity in experimental Parkinson's disease. *J Neurochem* **90**:1076–1084.
Liang LP, Pearson-Smith JN, Huang J, Day BJ, and Patel M (2019) Neuroprotective effects of a catalytic antioxidant in a rat nerve agent model. *Redox Biol* **20**:275–284.
McElroy PB, Liang LP, Day BJ, and Patel M (2017) Scavenging reactive oxygen species inhibits status epilepticus-induced neuroinflammation. *Exp Neurol* **298**:13–22.
Mogi M, Harada M, Kondo T, Riederer P, Inagaki H, Minami M, and Nagatsu T (1994a) Interleukin-1 beta, interleukin-6, epidermal growth factor and transforming growth factor-alpha are elevated in the brain from parkinsonian patients. *Neurosci Lett* **180**:147–150.
Mogi M, Harada M, Riederer P, Narabayashi H, Fujita K, and Nagatsu T (1994b) Tumor necrosis factor-alpha (TNF-alpha) increases both in the brain and in the cerebrospinal fluid from parkinsonian patients. *Neurosci Lett* **165**:208–210.
Müller T, Blum-Degen D, Przuntek H, and Kuhn W (1998) Interleukin-6 levels in cerebrospinal fluid inversely correlate to severity of Parkinson's disease. *Acta Neurol Scand* **98**:142–144.
Nagatsu T and Sawada M (2005) Inflammatory process in Parkinson's disease: role for cytokines. *Curr Pharm Des* **11**:999–1016.
Patel M (2016) Targeting oxidative stress in central nervous system disorders. *Trends Pharmacol Sci* **37**:768–778.
Paxinos G and Watson C (1995) *The Rat Brain in Stereotaxic Coordinates*, Academic Press, New York.
Perumal AS, Gopal VB, Tordzro WK, Cooper TB, and Cadet JL (1992) Vitamin E attenuates the toxic effects of 6-hydroxydopamine on free radical scavenging systems in rat brain. *Brain Res Bull* **29**:699–701.
Phani S, Loike JD, and Przedborski S (2012) Neurodegeneration and inflammation in Parkinson's disease. *Parkinsonism Relat Disord* **18** (Suppl 1):S207–S209.
Przedborski S and Jackson-Lewis V (1998) Mechanisms of MPTP toxicity. *Mov Disord* **13** (Suppl 1):35–38.
Przedborski S, Levivier M, Jiang H, Ferreira M, Jackson-Lewis V, Donaldson D, and Togasaki DM (1995) Dose-dependent lesions of the dopaminergic nigrostriatal pathway induced by intrastriatal injection of 6-hydroxydopamine. *Neuroscience* **67**: 631–647.
Sachs C and Jonsson G (1975) Mechanisms of action of 6-hydroxydopamine. *Biochem Pharmacol* **24**:1–8.
Sauer H and Oertel WH (1994) Progressive degeneration of nigrostriatal dopamine neurons following intrastriatal terminal lesions with 6-hydroxydopamine: a combined retrograde tracing and immunocytochemical study in the rat. *Neuroscience* **59**:401–415.
Sawa T, Akaike T, and Maeda H (2000) Tyrosine nitration by peroxynitrite formed from nitric oxide and superoxide generated by xanthine oxidase. *J Biol Chem* **275**: 32467–32474.
Sawada M, Imamura K, and Nagatsu T (2006) Role of cytokines in inflammatory process in Parkinson's disease. *J Neural Transm Suppl* (70):373–381.
Schapira AH, Cooper JM, Dexter D, Clark JB, Jenner P, and Marsden CD (1990) Mitochondrial complex I deficiency in Parkinson's disease. *J Neurochem* **54**:823–827.
Ungerstedt U and Arbuthnott GW (1970) Quantitative recording of rotational behavior in rats after 6-hydroxy-dopamine lesions of the nigrostriatal dopamine system. *Brain Res* **24**:485–493.
Ungerstedt U, Ljungberg T, and Steg G (1974) Behavioral, physiological, and neurochemical changes after 6-hydroxydopamine-induced degeneration of the nigrostriatal dopamine neurons. *Adv Neurol* **5**:421–426.
Uretsky NJ and Iversen LL (1970) Effects of 6-hydroxydopamine on catecholamine containing neurones in the rat brain. *J Neurochem* **17**:269–278.
Valko M, Leibfritz D, Moncol J, Cronin MT, Mazur M, and Telser J (2007) Free radicals and antioxidants in normal physiological functions and human disease. *Int J Biochem Cell Biol* **39**:44–84.
West MJ (1999) Stereological methods for estimating the total number of neurons and synapses: issues of precision and bias. *Trends Neurosci* **22**:51–61.
Wu DC, Jackson-Lewis V, Vila M, Tieu K, Teismann P, Vadseth C, Choi DK, Ischiropoulos H, and Przedborski S (2002) Blockade of microglial activation is neuroprotective in the 1-methyl-4-phenyl-1,2,3,6-tetrahydropyridine mouse model of Parkinson disease. *J Neurosci* **22**:1763–1771.
Yokoyama H, Uchida H, Kuroiwa H, Kasahara J, and Araki T (2011) Role of glial cells in neurotoxin-induced animal models of Parkinson's disease. *Neurol Sci* **32**:1–7.
Zhang S, Wang R, and Wang G (2019) Impact of dopamine oxidation on dopaminergic neurodegeneration. *ACS Chem Neurosci* **10**:945–953.
Zhang Y, Dawson VL, and Dawson TM (2000) Oxidative stress and genetics in the pathogenesis of Parkinson's disease. *Neurobiol Dis* **7**:240–250.
Zhou C, Huang Y, and Przedborski S (2008) Oxidative stress in Parkinson's disease: a mechanism of pathogenic and therapeutic significance. *Ann N Y Acad Sci* **1147**:93–104.

Address correspondence to: Dr. Manisha Patel, Department of Pharmaceutical Sciences, University of Colorado, Anschutz Medical Campus, 12850 East Montview Blvd., Aurora, CO 80045. E-mail: manisha.patel@cuanschutz.edu

Downloaded from jpet.aspetjournals.org at ASPET Journals on April 19, 2024